

Structural Effects of C₆ Substitution in 6-(4-(Dimethylamino)phenyl)fulvenes

Matthew L. Peterson, Jeffrey T. Strnad, Thomas P. Markotan, Carl A. Morales, Donald V. Scaltrito, and Stuart W. Staley*

Carnegie Mellon University, 4400 Fifth Avenue, Pittsburgh, Pennsylvania 15213

Received June 8, 1999

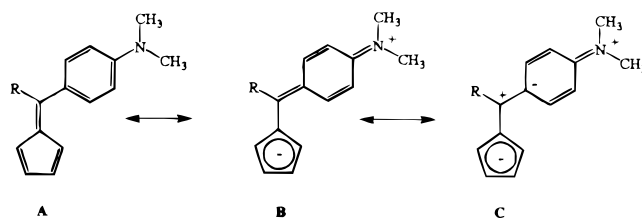
The single-crystal X-ray structures of 6-(4-(dimethylamino)phenyl)-6-methylfulvene (**2**) and of two polymorphs of 6-(4-(dimethylamino)phenyl)-6-phenylfulvene (**3**(*P2₁/c*) and **3**(*Pca2₁*)) have been determined and the structures of a series of 6-arylfulvenes (**1**–**8**) have been optimized at the HF/6-31G level. Analysis of these structures reveals how resonance and crystal lattice effects influence the degree of coplanarity between the aryl and fulvene rings. The torsional angles at the aryl–fulvene bonds are significantly larger in the optimized structures than in the X-ray structures. Natural bond orbital π charges and dipole moments calculated for the X-ray and optimized structures show that the crystalline environment enhances molecular polarization. Qualitative responses for second harmonic generation in powder samples have been observed in **2**, **3**(*Pca2₁*), and **5**. Compounds **2** and **3**(*Pca2₁*) have similar packing motifs despite packing in different space groups.

Introduction

The study of fulvene and substituted fulvenes¹ encompasses many areas of chemistry, including structure,^{2,3} NMR⁴ and electronic⁵ spectroscopy, reactivity,⁶ materials research,⁷ and the study of fundamental concepts such as polarity⁸ and aromaticity.⁹ Fulvene has been studied in the gas phase by microwave spectroscopy and found

to have alternating single and double bonds and to be only weakly polar ($\mu = 0.42$ D).^{3g} Substituted fulvenes have been shown to maintain this basic structural element, although structural perturbations suggestive of an increased importance of an “aromatic” five-membered ring have been observed.^{3e,f} In addition, substitution greatly increases the polarity of fulvene,^{8b} a response indicative of a highly polarizable moiety.²

Recent work has focused on the transmission of substituent effects through aryl spacers to the fulvene moiety from the standpoint of structure, charge distribution and chemical reactivity.^{2,4,6c,d,f,g,i,7b,8b} The relative importance of the resonance forms that describe the structure and electron distribution in these compounds has been discussed frequently over the years.



A significant increase in the second-order nonlinear optical response was found upon inclusion of a double-bond spacer between the aryl and fulvene rings.^{7a,d} Because π -electrons are more easily perturbed than σ -electrons, this work is indicative of long range π -electron communication in these compounds. However, a limited understanding of the electronic interactions in

(1) Reviews: (a) Yates, P. *Adv. Alicycl. Chem.* **1968**, *2*, 59. (b) Bergmann, E. D. *Chem. Rev.* **1968**, *68*, 41. (c) Lloyd, D. *Stud. Org. Chem.* **1984**, *16* (Nonbenzenoid Conjugated Carbocyclic Compounds).

(2) Wingert, L. M.; Staley, S. W. *Acta Crystallogr.* **1992**, *B48*, 782. (3) (a) Duda, L.; Erker, G.; Fröhlich, R.; Zippel, F. *Eur. J. Inorg. Chem.* **1998**, 1153. (b) Bolte, M.; Amon, M. *Acta Crystallogr.* **1997**, *C53*, 1354. (c) Teuber, R.; Köppe, R.; Linti, G.; Tacke, M. *J. Organomet. Chem.* **1997**, *545–546*, 105. (d) Rau, D.; Behrens, U. *J. Organomet. Chem.* **1990**, *387*, 219. (e) Ammon, H. L. *Acta Crystallogr.* **1974**, *B30*, 1731. (f) Böhme, R.; Burzlaff, H. *Chem. Ber.* **1974**, *107*, 832. (g) Baron, P. A.; Brown, R. D.; Burden, F. R.; Domaille, P. J.; Kent, J. E. *J. Mol. Spectrosc.* **1972**, *43*, 401. (h) Burzlaff, H.; Hartke, K.; Salamon, R. *Chem. Ber.* **1970**, *103*, 156. (i) Chiang, J. F.; Bauer, S. H. *J. Am. Chem. Soc.* **1970**, *92*, 261. (j) Norman, N.; Post, B. *Acta Crystallogr.* **1961**, *14*, 503.

(4) (a) Bircher, H.; Neuenschwander, M. *Helv. Chim. Acta* **1989**, *72*, 1697. (b) Bönzli, P.; Otter, A.; Neuenschwander, M.; Huber, H.; Kellerhals, H. P. *Helv. Chim. Acta* **1986**, *69*, 1052. (c) Sardella, D. J.; Keane, C. M.; Lemonias, P. J. *J. Am. Chem. Soc.* **1984**, *106*, 4962. (d) Otter, A.; Mühle, H.; Neuenschwander, M.; Kellerhals, H. P. *Helv. Chim. Acta* **1979**, *62*, 1626. (e) Pines, A.; Rabinovitz, M. *J. Chem. Soc. B* **1971**, 385.

(5) (a) Fabian, J.; Junek, H. *Dyes Pigments* **1985**, *6*, 251. (b) Griffiths, J.; Lockwood, M. *J. Chem. Soc., Perkin Trans. 1* **1976**, 48. (c) Weiss, R.; Murrell, J. N. *Tetrahedron* **1970**, *26*, 1131.

(6) (a) Nair, V.; Kumar, S. *Tetrahedron* **1996**, *52*, 4029. (b) Nair, V.; Kumar, S.; Anilkumar, G.; Nair, J. S. *Tetrahedron* **1995**, *51*, 9155. (c) Gugelchuk, M. M.; Chan, P. C.-M.; Sprules, T. J. *J. Org. Chem.* **1994**, *59*, 7723. (d) Gugelchuk, M.; Paquette, L. A. *J. Am. Chem. Soc.* **1991**, *113*, 246. (e) Chandrasekhar, S.; Venkatesan, V. *J. Chem. Res., Synop.* **1989**, 276. (f) Gugelchuk, M.; Paquette, L. A. *Isr. J. Chem.* **1989**, *29*, 165. (g) Paquette, L. A.; Gugelchuk, M. *J. Org. Chem.* **1988**, *53*, 1835. (h) Houk, K. N.; George, J. K.; Duke, R. E., Jr. *Tetrahedron* **1974**, *30*, 523. (i) Kresze, G.; Rau, S.; Sabelus, G.; Goetz, H. *Liebigs Ann. Chem.* **1961**, *648*, 57.

(7) (a) Kawabe, Y.; Ikeda, H.; Sakai, T.; Kawasaki, K. *J. Mater. Chem.* **1992**, *2*, 1025. (b) Kondo, K.; Goda, H.; Takemoto, K.; Aso, H.; Sasaki, T.; Kawakami, K.; Yoshida, H.; Yoshida, K. *J. Mater. Chem.* **1992**, *2*, 1097. (c) Papadopoulos, M. G.; Waite, J. *J. Chem. Soc., Faraday Trans.* **1990**, *86*, 3525. (d) Ikeda, H.; Kawabe, Y.; Sakai, T.; Kawasaki, K. *Chem. Phys. Lett.* **1989**, *157*, 576.

(8) (a) Replogle, E. S.; Trucks, G. W.; Staley, S. W. *J. Phys. Chem.* **1991**, *95*, 6908 and references cited; (b) Kresze, G.; Goetz, H. *Chem. Ber.* **1957**, *90*, 2161.

(9) (a) Tomas, X.; Andrade, J. M.; Alvarez-Larena, A. *Talanta* **1999**, *48*, 781. (b) Krygowski, T. M.; Cyrański, M. *Tetrahedron* **1996**, *52*, 1713. (c) Krygowski, T. M.; Ciesielski, A.; Cyrański, M. *Chem. Papers* **1995**, *49*, 128.

Table 1. X-ray Data for 2, 3(*P2₁/c*), and 3(*Pca2₁*)

	2	3(<i>P2₁/c</i>)	3(<i>Pca2₁</i>)
formula	C ₁₅ H ₁₇ N	C ₂₀ H ₁₉ N	C ₂₀ H ₁₉ N
formula wt (g/mol)	211.30	273.36	273.36
color and habit	orange square plates	orange blades	orange needles
cryst syst	orthorhombic	monoclinic	orthorhombic
<i>a</i> (Å)	7.426(2)	10.295(5)	30.890(6)
<i>b</i> (Å)	7.676(2)	12.257(5)	8.585(2)
<i>c</i> (Å)	21.694(4)	13.129(6)	5.850(1)
α (°)	90	90	90
β (°)	90	110.42(2)	90
γ (°)	90	90	90
<i>V</i> (Å ³)	1236.7(4)	1552.6(12)	1551.4(5)
<i>Z</i>	4	4	4
space grp	<i>P2₁2₁2₁</i>	<i>P2₁/c</i>	<i>Pca2₁</i>
<i>F</i> (000)	456	584	584
<i>D</i> (calcd) (g/cm ³)	1.135	1.169	1.170
cryst size (mm)	0.42 × 0.40 × 0.11	0.36 × 0.47 × 0.49	0.15 × 0.09 × 0.04
μ (mm ⁻¹)	0.496	0.067	0.511
collection range	-2 < <i>h</i> < 8 -2 < <i>k</i> < 8 -6 < <i>l</i> < 24	0 < <i>h</i> < 12 0 < <i>k</i> < 14 -15 < <i>l</i> < 14	0 < <i>h</i> < 34 0 < <i>k</i> < 9 -6 < <i>l</i> < 0
unique data measured	1102	2737	1295
obsd data	1099	1920	1294
no. of variables	162	248	209
<i>R</i>	0.0536	0.0453	0.0491
<i>wR</i> ²	0.1451	0.1275	0.0869

these compounds makes the optimization of technologically important properties difficult.

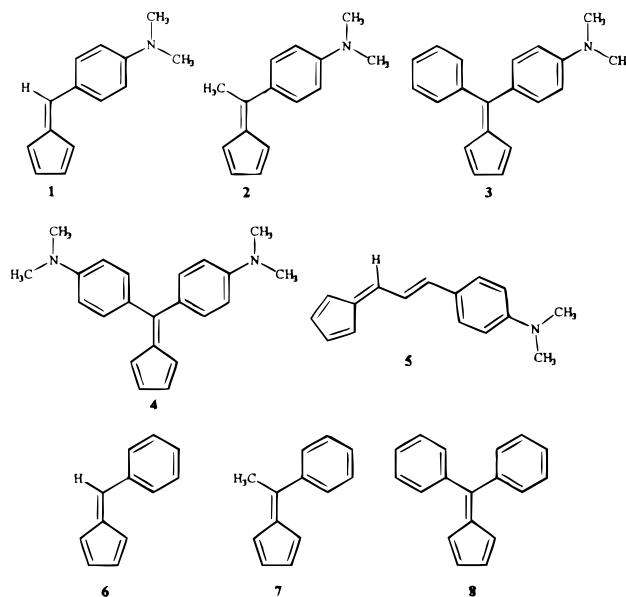
In the present study, we have determined the single-crystal X-ray structures of several strong donor-substituted fulvenes, 6-(4-(dimethylamino)phenyl)-6-methylfulvene (**2**) and two polymorphs of 6-(4-(dimethylamino)phenyl)-6-phenylfulvene (**3**). Steric and crystal packing effects have been elucidated by comparing the structures of similarly substituted compounds and by comparing the X-ray structures with HF/6-31G geometry-optimized structures. Finally, macroscopic nonlinear optical effects (second harmonic generation) have been evaluated qualitatively for several of these compounds.

Results

Single-crystal molecular structures for **2**, **3**(*P2₁/c*), and **3**(*Pca2₁*) were determined by X-ray diffraction. Synthetic details and procedures for crystal growth are given in the Experimental Section. Selected X-ray data for **1**,² **2**, **3**(*P2₁/c*), **3**(*Pca2₁*), and **4**^{3d} are given in Table 1, and complete data are collected in the Supporting Information. Selected X-ray bond lengths, bond angles and torsional angles for these compounds are listed in Tables 2–4, respectively. It should be noted that the X-ray structure of **1** was determined from a low-temperature data set while all of the other data collections were at ambient temperature. Hydrogen atoms were placed at idealized positions.

The molecular structures of **1–8** were optimized at the Hartree–Fock level using GAUSSIAN92¹⁰ or GAUSSIAN-94W¹¹ and the 6-31G¹² basis set and were checked by analytical frequency analysis. Optimization of **2** using the 6-31G*¹³ basis set showed only minor changes in structure and polarity (dipole moment). Selected bond lengths,

bond angles, and torsional angles for **1–8** are listed in Tables 5–7, respectively.



Frequency doubling of a 1064 nm laser beam was qualitatively observed for powder samples of **2**, **5**, and **3**(*Pca2₁*), although the latter compound showed only weak second harmonic generation (SHG). These experiments did not afford quantitative results because the NLO response depends on the crystal sizes as well as on the molecular response and crystal packing.¹⁴

Discussion

The major objective of this study is to elucidate the interdependence of π delocalization (π polarization and through resonance) and molecular structure in 6-phenyl- and 6-(4-(dimethylamino)phenyl)fulvenes and to determine how these effects are modified on incorporation into a crystal lattice. Because π delocalization is necessarily inextricably linked with steric effects of the other substituent at C₆, our approach to this problem is as follows. We have optimized the structures of **1–8** by ab initio molecular orbital theory at the Hartree–Fock (HF) level; these structures are appropriate for the isolated (“gas phase”) molecules. We have also determined the structures of **2** and **3** in the solid state by single-crystal X-ray diffraction, and the crystal structures of **1**, **4**, and **8** were

(10) Frisch, M. J.; Trucks, G. W.; Head-Gordon, M.; Gill, P. M. W.; Wong, M. W.; Foresman, J. B.; Johnson, B. G.; Schlegel, H. B.; Robb, M. A.; Replogle, E. S.; Gomperts, R.; Andres, J. L.; Raghavachari, K.; Binkley, J. S.; Gonzalez, C.; Martin, R. L.; Fox, D. J.; Defrees, D. J.; Baker, J.; Stewart, J. J. P.; Pople, J. A. *GAUSSIAN92*, Revision A; Gaussian, Inc., Pittsburgh, PA, 1992.

(11) Frisch, M. J.; Trucks, G. W.; Schlegel, H. B.; Gill, P. M. W.; Johnson, B. G.; Robb, M. A.; Cheeseman, J. R.; Keith, T. A.; Petersson, G. A.; Montgomery, J. A.; Raghavachari, K.; Al-Laham, M. A.; Zakrzewski, V. G.; Ortiz, J. V.; Foresman, J. B.; Cioslowski, J.; Stefanov, B. B.; Nanyakkara, A.; Challacombe, M.; Peng, C. Y.; Ayala, P. Y.; Chen, W.; Wong, M. W.; Andres, J. L.; Replogle, E. S.; Gomperts, R.; Martin, R. L.; Fox, D. J.; Binkley, J. S.; Defrees, D. J.; Baker, J.; Stewart, J. P.; Head-Gordon, M.; Gonzalez, C.; Pople, J. A. *GAUSSIAN-94W* (Revision 4.1); Gaussian, Inc., Pittsburgh, PA, 1995.

(12) Hehre, W. J.; Ditchfield, R.; Pople, J. A. *J. Chem. Phys.* **1972**, *56*, 2257.

(13) Hariharan, P. C.; Pople, J. A. *Chem Phys Lett.* **1972**, *16*, 217; Hariharan, P. C.; Pople, J. A. *Theor. Chim Acta* **1973**, *28*, 213.

(14) Nicoud, J. F.; Twieg, R. J. *Nonlinear Optical Properties of Organic Molecules and Crystals*; Chemla, D. S., Zyss, J., Eds.; Academic Press: New York, 1987; vol. 2, p 224 and references therein.

Table 2. Selected Bond Lengths for the X-ray Structures of 1–4^a

bonds ^b	1A ^c	1B ^c	2	3(P2 ₁ /c)	3(Pca2 ₁)	4
Dbl = C ₁ C ₂ , C ₃ C ₄	1.355(2)	1.354(2)	1.338(5)	1.334(3)	1.36(1)	1.347(2)
Sngl = C ₅ C ₁ , C ₂ C ₃ , C ₄ C ₅	1.461(2)	1.467(2)	1.458(2)	1.454(2)	1.44(1)	1.448(2)
C ₅ C ₆	1.364(3)	1.362(2)	1.366(5)	1.363(3)	1.37(1)	1.366(3)
C ₆ C ₇	1.451(3)	1.456(2)	1.465(5)	1.472(3)	1.46(1)	1.472(2)
C ₆ C ₁₃				1.482(3)	1.49(1)	1.474(2)
b = C ₈ C ₉ , C ₁₁ C ₁₂	1.372(2)	1.377(2)	1.377(4)	1.370(2)	1.39(1)	1.377(2)
a = C ₇ C ₈ , C ₉ C ₁₀ , C ₁₀ C ₁₁ , C ₁₂ C ₇	1.412(1)	1.413(1)	1.398(3)	1.398(2)	1.40(1)	1.401(1)
b = C ₁₄ C ₁₅ , C ₁₇ C ₁₈				1.379(2)	1.37(1)	1.376(2)
a = C ₁₃ C ₁₄ , C ₁₅ C ₁₆ , C ₁₆ C ₁₇ , C ₁₈ C ₁₃				1.380(2)	1.37(1)	1.396(2)
C ₁₀ N	1.373(2)	1.376(2)	1.368(3)	1.372(2)	1.40(1)	1.369(2) ^d
Δ(Sngl – Dbl)	0.106	0.113	0.120	0.120		0.101
Δ(a – b)	0.040	0.036	0.021	0.028	0.01	0.024
						0.020 ^e

^a In Å. ^b The value given where more than one bond is listed is the average value. ^c There are two crystallographically independent molecules. ^d Both CN bonds are the same length. ^e Value for the second *p*-(dimethylamino)phenyl ring.

Table 3. Selected Bond Angles for the X-ray Structures of 1–4^a

bond angle	1A ^b	1B ^b	2	3-(P2 ₁ /c)	3-(Pca2 ₁)	4
C ₁ C ₅ C ₆	132.6(2)	132.9(2)	128.4(2)	126.8(2)	130(1)	127.7(2)
C ₄ C ₅ C ₆	121.9(2)	121.8(2)	126.1(3)	128.3(2)	123(1)	127.1(2)
C ₅ C ₆ C ₇	131.9(2)	132.5(2)	123.4(2)	122.9(2)	124(1)	121.7(2)
C ₅ C ₆ C ₁₃			120.3(3)	121.0(2)	120(1)	122.8(2)
C ₁ C ₅ C ₄	105.5(2)	105.2(2)	105.4(3)	104.9(2)	107(1)	105.1(2)
C ₆ C ₁₃ C ₁₄				120.9(2)	119(1)	123.4(2)
C ₆ C ₇ C ₈	125.8(2)	127.0(2)	121.9(2)	121.0(2)	123(1)	122.9(2)
C ₈ C ₇ C ₁₂	116.5(2)	116.1(2)	115.7(2)	116.5(2)	115(1)	115.9(2)
						116.4(2) ^c
C ₉ C ₁₀ C ₁₁	117.4(2)	117.3(2)	116.6(3)	116.6(3)	119(1)	117.0(2)
						116.6(2) ^d
∠T ^e	10.7	11.1	2.3	–1.5	7	0.6

^a In degrees. ^b There are two crystallographically independent molecules. ^c ∠C₁₄C₁₃C₁₈. ^d ∠C₁₅C₁₆C₁₇. ^e Reference 17.

Table 4. Selected Torsional Angles for the X-ray Structures of 1–4^a

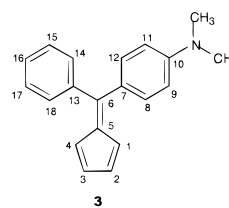
torsional angle	1A ^b	1B ^b	2	3(P2 ₁ /c)	3(Pca2 ₁)	4
ωC ₅ C ₆	3.1	2.5	7.2	11.9	10	11.0
ωC ₆ C ₇	13.2	13.8	32.7	37.4	28	36.0
ωC ₆ C ₁₃				49.2	60	45.3
ωC ₁₀ N ₁	7.0	3.5	3.7	4.2	10	2.4
						7.6 ^c

^a In degrees; the parameters ω(C₆C₇), ω(C₅C₆), ω(C₆C₁₃), ω(C₁₀N), and ω(C₁₆N) are defined as the average of the torsional angles, excluding those involving hydrogen, at a given bond. Angles larger than 90° were subtracted from 180° before averaging. ^b There are two crystallographically independent molecules. ^c Value for the second *p*-(dimethylamino)phenyl ring.

retrieved from the Cambridge Structural Database (CSD).¹⁵ Comparison of compounds with different substituents at C₆ and of phenyl vs *p*-(dimethylamino)phenyl substitution provides insight into the relative contributions of steric and π delocalization effects.

We next analyze the structural changes that occur on incorporating 1–4 into a crystal lattice by comparing calculated structures with X-ray structures. We also have been able to obtain and structurally characterize two polymorphs of 3. Comparison of these polymorphs and, more generally, of compounds possessing similar or different crystal packing motifs provides additional information about the role of the crystal lattice. In the final section, we qualitatively relate the solid-state structures of these compounds with SHG, a potential technologically important property of these compounds.

(15) 3D Search and Research Using the Cambridge Structural Database. Allen, F. H.; Kennard, O. *Chem. Design Automation News* 1993, 8, 1, 31.

Chart 1

Molecular Structures. Important structural parameters for HF/6-31G geometry-optimized structures and for X-ray structures of 6-(4-(dimethylamino)phenyl)fulvenes 1–4 as well as for 6-phenylfulvenes 6–8 are given in Tables 2–7. In each case, the bonds from the central carbon atom (C₆) to the attached rings are twisted in the same sense so that 6,6-diarylfulvenes 3, 4, and 8 assume a propeller-like shape. (See Chart 1 for numbering.) The largest parameter changes are observed for the average torsional angle at the C₆C₇ bond (ω(C₆C₇)),¹⁶ which varies over a range of nearly 30° in the calculated structures and over 40° in the solid state (Tables 7 and 4, respectively) and represent a measure of the twisting between the (dimethylamino)phenyl ring and the fulvene ring. The value of ω(C₆C₇) increases in the order 6 < 8 = 3 < 7 for compounds with a 6-phenyl group and in the order 1 < 3 = 4 < 2 for those with a 6-*p*-(dimethylamino)phenyl group. Thus, the “steric size” of the C₆ substituent increases in the order H < Ph = C₆H₄NMe₂ < Me. We attribute the slightly smaller steric size of phenyl and (dimethylamino)phenyl relative to methyl in these compounds to the ability of adjacent aryl groups to rotate in the same sense in order to minimize repulsive interactions.

Comparison of ω(C₆C₇) for phenyl in 6, 7, 3, and 8 with (dimethylamino)phenyl in 1, 2, 3, and 4, respectively (replacement of phenyl with (dimethylamino)phenyl), indicates that the latter ring is less twisted by 5–7° in the calculated structures and by 3–7° in the X-ray structures. This is strong evidence for a greater resonance effect for (dimethylamino)phenyl relative to phenyl. Sardella et al. previously concluded that there is relatively little resonance interaction in 6-aryl-6-methylfulvenes on the basis of ¹³C chemical shifts.^{4c} However, close examination of their data reveals a significant contribution for resonance.^{4c}

(16) The parameters ω(C₆C₇), ω(C₅C₆), and ω(C₆C₁₃) are defined as the average of the torsional angles, excluding those involving hydrogen, at a given bond. Angles larger than 90° were subtracted from 180° before averaging.

Table 5. Selected Bond Lengths for HF/6-31G-Optimized Structures of 1–8^a

bonds ^b	1	2	3	4	5	6	7	8
Dbl = C ₁ C ₂ , C ₃ C ₄	1.3431	1.3429	1.3434	1.3450	1.3437	1.3412	1.3417	1.3420
Sngl = C ₅ C ₁ , C ₂ C ₃ , C ₄ C ₅	1.4735	1.4746	1.4743	1.4721	1.47180	1.4765	1.4764	1.4765
C ₅ C ₆	1.3420	1.3462	1.3507	1.3540	1.3433	1.3384	1.3428	1.3474
C ₆ C ₇	1.4651	1.4882	1.4851	1.4861	1.4484	1.4733	1.4937	1.4922
C ₆ C ₁₃			1.4931	1.4861	1.4634 ^d			
b = C ₈ C ₉ , C ₁₁ C ₁₂	1.3805	1.3823	1.3815	1.3818	1.3801	1.3858	1.3868	1.3865
a = C ₇ C ₈ , C ₉ C ₁₀ , C ₁₀ C ₁₁ , C ₁₂ C ₇	1.4003	1.3985	1.3995	1.3994	1.4002	1.3921	1.3910	1.3915
b = C ₁₄ C ₁₅ , C ₁₇ C ₁₈			1.3866	1.3817				1.3865
a = C ₁₃ C ₁₄ , C ₁₅ C ₁₆ , C ₁₆ C ₁₇ , C ₁₈ C ₁₃			1.3915	1.3994				1.3915
C ₁₀ N	1.3814	1.3836	1.3821	1.3829				
Δ(Sngl – Dbl)	0.1304	0.1317	0.1309	1.1271	0.1281	0.1353	0.1347	0.1345
Δ(a – b)	0.0198	0.0162	0.0181	0.0176	0.0200	0.0063	0.0041	0.0050
			0.0049 ^e	0.0176 ^e				0.0050 ^f

^a In Å. ^b The value given where more than one bond is listed is the average value. ^c Length of the ethendiyl bond. ^d Length of the single bond between the ethendiyl group and the aryl ring. ^e Values for phenyl ring. ^f Value for the second *p*-(dimethylamino)phenyl ring.

Table 6. Selected Bond Angles for HF/6-31G-Optimized Structures of 1–8^a

bond angle	1	2	3	4	5	6	7	8
C ₁ C ₅ C ₆	130.7	127.4	127.6	127.5	129.1	130.3	127.3	127.5
C ₄ C ₅ C ₆	124.1	127.8	127.4	127.5	125.4	124.5	127.5	127.5
C ₅ C ₆ C ₇	129.4	122.4	122.5	121.8	126.6 ^b	128.4	122.0	122.0
C ₅ C ₆ C ₁₃		122.5	121.3	121.8			123.2	122.0
C ₁ C ₅ C ₄	105.2	104.8	105.0	105.0	105.4	105.2	104.9	105.0
C ₆ C ₁₃ C ₁₄			121.1	121.2				120.3
C ₆ C ₇ C ₈	123.8	121.5	122.0	121.92	122.4 ^c	122.6	120.8	121.2
C ₈ C ₇ C ₁₂	116.8	116.8	116.9	116.92	116.6	118.4	118.5	118.5
				116.92 ^d				
C ₉ C ₁₀ C ₁₁	117.2	117.1	117.2	117.22	117.1	119.6	119.6	119.6
				117.22 ^e				
∠T ^f	6.6	−0.4	0.2	0.0	3.7	5.8	−0.2	0.0

^a In degrees. ^b Angle formed by atoms C₅, C₆ and the ethendiyl carbon attached to C₆. ^c Angle formed by the ethendiyl carbon atoms and C₇. ^d ∠C₁₄C₁₃C₁₈. ^e ∠C₁₅C₁₆C₁₇. ^f Reference 17.

Table 7. Selected Torsional Angles for HF/6-31G-Optimized Structures of 1–8^a

torsional angle	1	2	3	4	5	6	7	8
ωC ₅ C ₆	4.4 ^b	5.3 ^c	9.9	11.4	0.0	3.5	3.4	8.4
ωC ₆ C ₇	30.4 ^b	51.8 ^c	45.3	45.5	0.0	37.0	58.9	50.0
ωC ₆ C ₁₃			50.2	45.5				50.0
ωC ₁₀ N ₁	0.9	0.6	0.6	0.3	0.0			
ωC ₁₆ N ₂				0.5	0.0			

^a In degrees; the parameters ω(C₆C₇), ω(C₅C₆), ω(C₆C₁₃), ω(C₁₀N), and ω(C₁₆N) are defined as the average of the torsional angles, excluding those involving hydrogen, at a given bond. Angles larger than 90° were subtracted from 180° before averaging. ^b Values of ω(C₅C₆) and ω(C₆C₇) of 2.6° and 33.2°, respectively, were calculated for **1** at HF/STO-3G (ref 2). Values of ω(C₅C₆) and ω(C₆C₇) of 13.1° and 36.0°, respectively, were calculated for **2** at a DFT/JMW/double numeric plus polarization level (ref 6c). However, these values were not confirmed by analytical frequency analysis.

Comparison of the calculated structures for **3** and **8** with the corresponding X-ray structures indicates that the twist of the phenyl group is essentially unchanged on incorporation into the solid state. In contrast, the twist of the (dimethylamino)phenyl group decreases in the solid state by 17–19° in **1**, **2**, and **3**(*Pca2*₁) and by 8–10° in **3**(*P2*₁/*c*) and **4**. These results strongly suggest an enhanced π-delocalization in the solid state. This is supported by HF/6-31G calculations of the dipole moments (μ) for **1–4** at the optimized geometries and at the X-ray structures (Table 8). In each case, μ increases by 0.56–1.32 D on going to the X-ray structure. The crystal lattice is expected to cause additional polarization. As discussed in the next section, these changes are influenced not only

Table 8. Calculated Dipole Moments for 1–4

compd	dipole moment ^a		
	optimized structure ^b	X-ray structure ^c	difference ^{a,d}
1A	3.94	5.07	1.13
1B	3.94	5.09	1.15
2	3.66	4.99	1.33
3 (<i>P2</i> ₁ / <i>c</i>)	3.76	4.38	0.62
3 (<i>Pca2</i> ₁)	3.76	4.32	0.56
4	4.63	5.76	1.13

^a In D. ^b HF/6-31G//HF/6-31G. ^c HF/6-31G//X-ray. ^d μ(X-ray) – μ(optimized).

by the solid state in general but also by the specific crystal packing motif that is employed.

Another parameter that can be employed to assess relative steric size is ∠T = ∠C₁C₅C₆ – ∠C₄C₅C₆ (Tables 3 and 5), which is a measure of the “tilt” of the exocyclic fulvene double bond toward the smaller of the two substituents at C₆.¹⁷ When the second substituent at C₆ is phenyl (**3**, **6–8**) or (dimethylamino)phenyl (**1–4**), ∠T in the calculated structures increases in the order H < Ph ≤ C₆H₄NMe₂ < Me. This is the same order as determined from ω(C₆C₇). In contrast, ∠T in the X-ray structures of **1–4** increases in the order H < Me < Ph < C₆H₄NMe₂ when the second substituent at C₆ is (dimethylamino)phenyl. This occurs in response to the above-mentioned “flattening” of the (dimethylamino)phenyl ring, which causes an increase in its steric size.

The torsion at the C₅C₆ bond (ω(C₅C₆))¹⁶ increases in the order **1** < **2** < **3** < **4** (H < Me < Ph < C₆H₄NMe₂) (Tables 4 and 7). Note that here also the effect of methyl is less than that of aryl, in contrast to the order for ω(C₆C₇). We suggest that this is due to a greater stabilization by aryl (relative to methyl) of resonance forms **B** and **C**, which contribute single bond character to the C₅C₆ double bond. Strong evidence for the role of π delocalization in these compounds is also given by (a) a very good linear correlation (*r*² = 0.91) for a plot of the C₆C₇ bond length (*r*(C₆C₇)) vs ω(C₆C₇) (Figure 1), as would be expected from a contribution of through-resonance form **B** and (b) the NMR chemical shifts of C₆, which increase in the order **1** (139.9 in CDCl₃)² < **2** (150.6 in CDCl₃) < **3** (153.4 in THF-*d*₈), in accord with an increased contribution of π polarization (resonance form **C**).

The value of *r*(C₆C₇) decreases by ca. 0.007 Å in the “gas phase” and by 0.1–0.2 Å in the crystal on changing

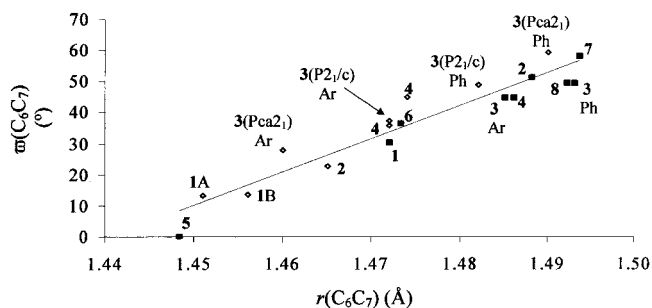


Figure 1. Plot of $\omega(\text{C}_6\text{C}_7)$ vs $r(\text{C}_6\text{C}_7)$ or $\omega(\text{C}_6\text{C}_{13})$ vs $r(\text{C}_6\text{C}_{13})$ for calculated structures (■) of **1–8** and X-ray structures (◇) of **1–4** ($r^2 = 0.91$). In cases where both phenyl and *p*-(dimethylamino)phenyl substituents are present (**3**, **3**(*P2*_{1/c}), and **3**(*Pca2*₁)), the labels Ph and Ar, respectively, are employed.

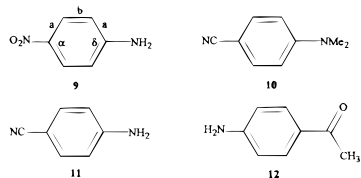
Table 9. Average X-ray Bond Lengths of Phenylene Bonds a and b and Their Difference^a

compd	r_a	r_b	$\Delta(r_a - r_b)$	compd	r_a	r_b	$\Delta(r_a - r_b)$
1	1.413	1.375	0.038	9^b	1.401	1.374	0.027
2	1.398	1.377	0.021	10^c	1.391	1.372	0.019
3 (<i>P2</i> _{1/c})	1.398	1.370	0.028	11^d	1.401	1.372	0.029
4	1.401	1.377	0.024	12^e	1.396	1.369	0.027

^a In Å; bonds a and b are defined in structure **9**. ^b Average values for three structures (ref 18). ^c Average values for five structures (ref 19). ^d Average values for two structures (ref 19a, 20). ^e Reference 21.

from Ph to C₆H₄NMe₂ (Tables 5 and 2, respectively), again reflecting the greater resonance effect of the latter. Further, $r(\text{C}_6\text{C}_7)$ for C₆H₄NMe₂ decreases by 0.011–0.023 Å in **1–4** on incorporation into the crystal, in contrast to changes of –0.011 and +0.002 Å for Ph in **3** and **8**, respectively. This indicates that C₆H₄NMe₂ is more polarized in the solid state (relative to the gas phase) than is Ph.

Another indicator of resonance is provided by the quinoid character of the C₆ aryl ring (as illustrated by structures **B** and **C**). The difference (for X-ray structures) between the average length of the “end” bonds (a) and the “side” bonds (b) (see **9** and Table 9) is 0.038, 0.021, 0.028, and 0.024 Å for **1**, **2**, **3**(*P2*_{1/c}) and **4**, respectively. This is about the same magnitude as found for the average difference (0.026 Å) in four strong donor/strong acceptor (D/A)-substituted benzenes, **9**,¹⁸ **10**,¹⁹ **11**,^{19a,20} and **12**.²¹



(18) (a) Tonogaki, M.; Kawata, T.; Ohba, S.; Iwata, Y.; Shibuya, I. *Acta Crystallogr.* **1993**, *B49*, 1031. (b) Colapietro, M.; Domenicano, A.; Marciante, C.; Portalone, G. *Z. Naturforsch.* **1982**, *37B*, 1309. (c) Trueblood, K. N.; Goldish, E.; Donohue, J. *Acta Crystallogr.* **1961**, *14*, 1009.

(19) (a) Jameson, G. B.; Sheikh-Ali, B. M.; Weiss, R. G. *Acta Crystallogr.* **1994**, *B50*, 703. (b) Heine, A.; Herbst-Irmer, R.; Stalke, D.; Kühnle, W.; Zachariasse, K. A. *Acta Crystallogr.* **1994**, *B50*, 363. (c) Gourdon, A.; Launay, J.-P.; Bujoli-Doeuff, M.; Heisel, F.; Miché, J. A.; Amouyal, E.; Boillot, M.-L. *J. Photochem. Photobiol. A: Chem.* **1993**, *71*, 13.

(20) Merlino, S.; Sartori, F. *Acta Crystallogr.* **1982**, *B38*, 1476.

(21) Haisa, M.; Kashino, S.; Yuasa, T.; Akigawa, K. *Acta Crystallogr.* **1976**, *B32*, 1326.

Table 10. X-ray Bond Angles in Phenylene Rings^a

compd	α	δ	compd	α	δ	$\Delta\alpha^b$	$\Delta\delta^b$
1	116.3	117.3	8^d	118.6	119.9		
2	115.7	116.9	9^e	121.1	118.7	–0.5	–0.5
3 (<i>P2</i> _{1/c})	116.5	116.9	10^f	118.3	117.1	1.1	0.4
3 (<i>P2</i> _{1/c}) ^c	118.0	119.7	11^g	119.2	118.6	0.6	0.1
4	116.2	116.8	12^h	116.7	118.1	1.0	0.4

^a Angles α and β (defined in structure **9**); in degrees. ^b Difference between the predicted^{22a} and average X-ray bond angles. ^c Values for the phenyl ring in **3**(*P2*_{1/c}). ^d Reference 3b; no atomic coordinates were available for the structure reported in ref 3c. ^e Average values for three structures (ref 18). ^f Average values for five structures (ref 19). ^g Average values for two structures (ref 19a, 20). ^h Reference 21.

The angles α and δ (see **9**) have previously been employed to evaluate the effect of substituents on substituted benzenes in the solid state. Domenicano and co-workers have compiled an extensive list of “angular substituent parameters” (ASPs) that allow one to predict the ability of a substituent to distort CCC angles from the benzene value of 120°. These angles are primarily determined by changes in the σ bonds due to the effect of the electronegativity of the substituent on the hybridization of the ring carbon to which it is bonded. However, as recognized by these workers, the contribution of π -resonance effects will tend to shorten the C₁-substituent bond and decrease α for both donors and acceptors.²³ Thus, the deviation of the measured value of α from the value predicted from ASPs can be taken to be an indication of the contribution of through resonance to the structure of a given para-disubstituted benzene.

The deviations of the average X-ray values of α and δ in **1–4** (for C₆H₄NMe₂), **3** and **8** (for Ph) and in D/A-substituted benzenes **9–12** from the values predicted from the ASPs are given in Table 10. Note that the deviations for phenyl are small and positive (i.e., in the opposite direction expected for resonance). In contrast, *p*-(dimethylamino)phenyl shows a negative deviation, but one that is half or less than those shown by strong D/A-benzenes **9–12**. This suggests that 6-(4-(dimethylamino)phenyl)fulvenes have significant through-resonance contributions, but less than found in **9–12**. The twist between the aryl and fulvene rings in **1–4** undoubtedly accounts, at least in part, for the smaller ASP deviations found in these compounds.

An analysis of the effects on molecular structure brought about by incorporation into a crystal lattice was previously presented for **1** (which had been optimized at the HF/STO-3G level), and the following changes were noted.² (1) The interplanar angle between the fulvene and aryl rings is reduced in the crystal with respect to its calculated value. (2) The pyramidalization of the dimethylamino group is largely (but not completely) eliminated in the X-ray structure. (This is not true for the compounds discussed here since the dimethylamino group is not significantly pyramidalized in the structures optimized using the 6-31G basis set.) (3) The “tilt angle” ($\angle T$) is increased. (4) The length of the C₅C₆ bond ($r(\text{C}_5\text{C}_6)$) is increased while $r(\text{C}_6\text{C}_7)$ is reduced by a similar amount. (5) The average single bond length in the fulvene ring is reduced in the crystal. (6) The bond lengths of

(22) (a) Domenicano, A. *Methods Stereochem. Anal.* **1988**, *10* (Stereochem. Appl. Gas-Phase Electron Diff., Part B), 281. (b) Domenicano, A.; Murray-Rust, P. *Tetrahedron Lett.* **1979**, 2283.

(23) Domenicano, A.; Viciago, A.; Coulson, C. A. *Acta Crystallogr.* **1975**, *B31*, 221.

the (dimethylamino)phenyl ring change to reflect a more quinoid shape for the ring (as in **B** and **C**). (7) The bonds to N, particularly C₁₀N, are shortened. It can be seen in Tables 2–7 that all of these trends, except point 2 as explained above, are also present in **2**, **3** (*Pca2₁*), and **4** when the X-ray structures are compared with the corresponding HF/6-31G-optimized structures.

Crystal Packing. In most crystalline aromatic compounds lacking strong hydrogen bond donors and acceptors, the major intermolecular binding forces are dispersion/electrostatic in nature. The latter are commonly manifested as edge-to-face interactions between the hydrogen periphery of one molecule and the π -cloud of an adjacent molecule.²⁴ It has been shown statistically that the magnitude of the molecular dipole moment is not related to bulk centrosymmetry (or noncentrosymmetry) in the crystalline form.²⁵ It has also been noted that only slight misalignments of adjacent dipoles are necessary to cause noncentrosymmetry.²⁶ These misalignments probably do not have a large influence on the nature of the basic intermolecular interactions. The molecules are still oriented so that their dipole moments are aligned in nearly opposite directions and the important electrostatic (edge-to-face) interactions are basically the same. A study of the relationship between local dipole moments and head-to-tail packing arrangements showed that the latter become more important as the local dipole moments are brought closer together.²⁶

We have previously discussed the relationship of dipole–dipole alignment to crystal packing in **1**.² The molecules align in a herringbone fashion with molecular dipoles in adjacent layers pointing in opposite directions. By packing in this way, molecular dipole moments are enhanced through interactions with the dipole moments of neighboring molecules. Both $\omega_{C_5C_6}$ and $\omega_{C_6C_7}$ are smaller (by $\sim 1.5^\circ$ and $\sim 16.8^\circ$, respectively) in the crystal than in the optimized structures, suggesting that μ is increased in the crystal.

A. 6-(4-(Dimethylamino)phenyl)-6-methylfulvene (2). Compound **2** packs in space group *P2₁2₁2₁* with four molecules per asymmetric unit. The molecules pack so that the local dipole moments of the aryl rings are aligned in a head-to-tail arrangement (type I, Figures 2 and 3) with close contacts of 3.2 Å between H₉ and C₁₀ or N. The aryl rings packing in this manner form a pentamer with the angle between the central aryl ring and the surrounding aryl rings being 58°. Two of the neighboring molecules are offset more than the other two, the distances between the centroids of the central aryl ring and the corresponding centroids of the two pairs of neighbors being 5.2 and 5.7 Å. The shorter centroid–centroid distance involves the more offset aryl rings. This arrangement leads to stacks of molecules along the *b* axis with interleaved aryl rings, the distance between the stacks being 7.67 Å, approximately the same as the sum of the van der Waals radii for a methyl group and a phenylene ring (7.7 Å²⁷). Thus, the alignments of the local dipole moments along the C₁₀–N bond could enhance the donation of π -electron density from the nitrogen to the aryl ring.

(24) (a) Hunter, C. A. *Chem. Soc. Rev.* **1994**, 101. (b) Hunter, C. A.; Sanders, J. K. M. *J. Am. Chem. Soc.* **1990**, *112*, 5525.

(25) Whitesell, J. K.; Davis, R. E.; Saunders, L. L.; Wilson, R. J.; Feagin, J. P. *J. Am. Chem. Soc.* **1991**, *113*, 3267.

(26) Gavezzotti, A. *J. Phys. Chem.* **1990**, *94*, 4319.

(27) Dunitz, J. D. *X-ray Analysis and the Structure of Organic Molecules*; VCH: New York, 1995; p 339.

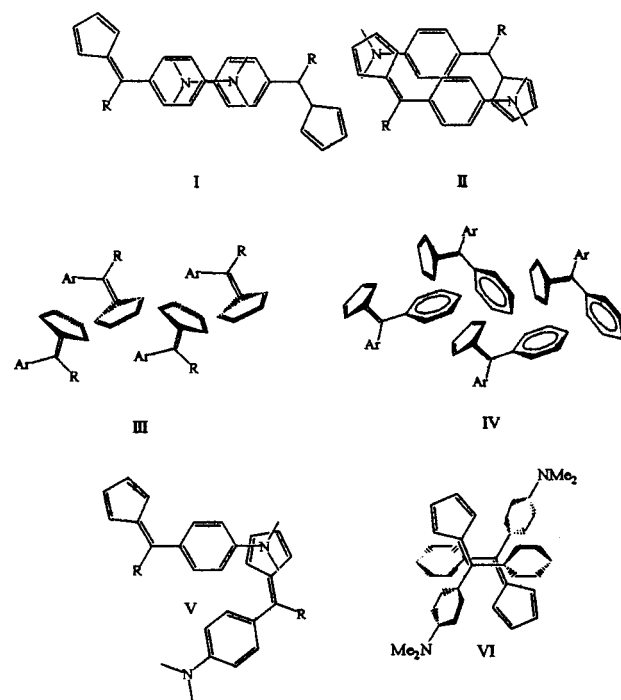


Figure 2. Packing motifs for **1–4**.

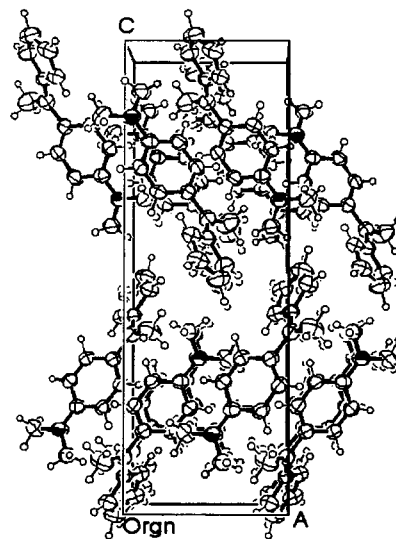


Figure 3. Packing diagram for **2**.

The fulvene ring in **2** also packs in a head-to-tail manner (type III, Figure 3) with respect to neighboring fulvene rings (intermolecular interplanar angle between fulvene rings = 75.6°). The contacts between fulvene rings are edge-to-face in nature with C₁⋯H₄, C₂⋯H₄, and C₅⋯H₄ having intermolecular distances of 2.8, 3.0, and 3.2 Å, respectively.²⁸ This arrangement aligns the dipole moments of adjacent fulvene rings in opposite directions.

These two types of head-to-tail intermolecular interactions between local dipoles act in concert to polarize the molecule in the crystal and contribute to a decrease in $\omega_{C_6C_7}$ of 19.1° relative to that in the optimized structure. The fact that $\omega_{C_5C_6}$ is 1.9° larger in the crystal than in

(28) It was recently pointed out that intermolecular interactions need not be energetically stabilizing. The intermolecular interactions shown in italics may be destabilizing: Dunitz, J. D.; Gavezzotti, A. *Acc. Chem. Res.* **1999**, *32*, 677.

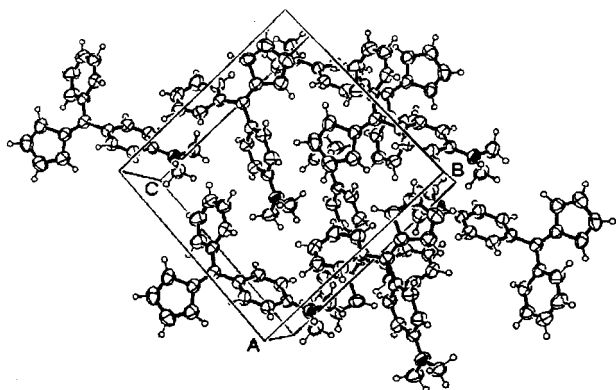


Figure 4. Packing diagram for **3**(*P2₁/c*).

the optimized structure of **2** is indicative of a greater importance of resonance forms **B** and/or **C** in the crystal and/or an increase in steric effects arising from the decrease in $\omega(\text{C}_6\text{C}_7)$. Increased molecular polarization in the crystal was confirmed by an increase in μ (Table 8) as well as the π charges at C_{1–6} (Supporting Information) calculated at the HF/6-31G level and the X-ray geometry (HF/6-31G//X-ray).

B. 6-(4-(Dimethylamino)phenyl)-6-phenylfulvene (3(P2₁/c)). Several different packing interactions are apparent in this compound (Figure 4). There are π -to- π stacks between phenyl and fulvene rings (type VI, Figure 2) where the phenyl ring of one molecule sits over C₁ and C_{5–8} of a neighboring molecule. H₂₀ is involved in intermolecular close contacts with C₁, C₅, and C₆ of 2.8, 3.2, and 3.3 Å, respectively,²⁸ and the phenyl and fulvene rings are inclined by 21.7° degrees with respect to one another. Since the two molecules are related by a center of symmetry, the molecular μ 's are parallel and aligned in opposite directions. In addition to the π -to- π stacks, the fulvene ring of each molecule is sandwiched between the dimethylamino groups of two neighboring molecules such that the molecular dipole moments align in a herringbone motif (type V, Figure 2). One methyl hydrogen (H₁₉) is involved in three intermolecular close contacts with C₃, C₄ and C₅ of 3.1, 3.2, and 3.2 Å, respectively, and another (H₂₀) is involved in two intermolecular close contacts with C₁ and C₅ of 2.8 and 3.2 Å, respectively.²⁸ This arrangement places the positive end of one molecular dipole moment near the negative end of a neighbor. There is one head-to-tail (type I, Figure 2) interaction between aryl rings parallel to each other with a C₁₀...N distance of 3.65 Å.

C. 6-(4-(Dimethylamino)phenyl)-6-phenylfulvene (3(Pca2₁)). The packing here appears to be dominated by type-I interactions. The nitrogen on one aryl group sits over a neighboring aryl ring such that the local dipoles of the (dimethylamino)phenyl rings are aligned antiparallel to one another (Figure 5). H₂₀ is in close contact (2.8 Å)²⁸ with both C₁ and C₂. The molecules packed in this way form bilayers in the *bc* plane. The planes of the aryl rings are tilted by 55° with respect to one another and are also offset from one another.

By packing into bilayers, each aryl ring is surrounded by four neighboring aryl rings aligned in antiparallel directions similar to the packing motif found in **2**. The molecular bilayers are stacked with respect to a neighboring bilayer so that the fulvene and phenyl rings of one molecule are aligned head-to-head with those of a

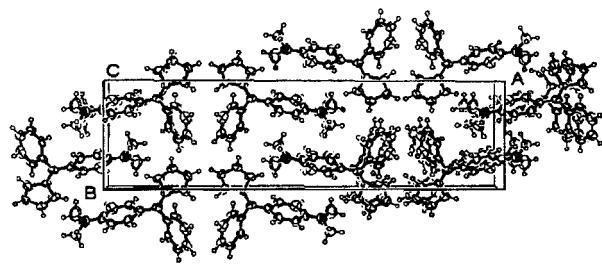


Figure 5. Packing diagram for **3**(*Pca2₁*).

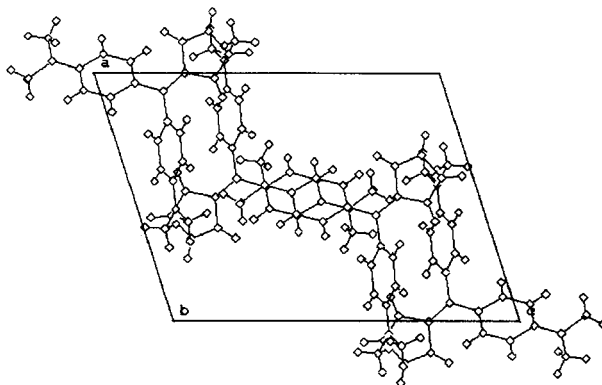


Figure 6. Packing diagram for **4**.

neighboring bilayer (type IV, Figure 2). The neighboring fulvene rings are inclined by 6.1° relative to one another while the intermolecular interplanar angle between neighboring phenyl rings is 75.1°.

The most notable difference between the packing of polymorphs **3**(*P2₁/c*) and **3**(*Pca2₁*) is that there is only one type-I interaction per molecule in the former compared to four such interactions in the latter. This difference is undoubtedly related to the differences in molecular conformation between the two polymorphs. The value of $\omega(\text{C}_6\text{C}_7)$ is 10° smaller in **3**(*Pca2₁*) than in **3**(*P2₁/c*), suggesting that the local μ of the former is larger.

D. 6,6-Bis(4-(dimethylamino)phenyl)fulvene (4).^{3d} Another indication of the influence of crystal packing on the molecular structure of these compounds can be seen in **4**. The two aryl rings in the calculated structure of **4** are equivalent. However, in the crystal one aryl ring is more twisted relative to the fulvene ring than the other (Table 7). The more coplanar aryl ring has one type I interaction with the more coplanar aryl ring of an adjacent molecule in the crystal (Figure 6). The intermolecular interplanar angle in this case is 0.0°. The other aryl ring (larger $\omega\text{C}_6\text{C}_{Ar}$) is involved in a type-II interaction (Figure 2) with the hydrogens of one aryl ring lying over the π -system of the adjacent aryl ring (aryl-aryl interplanar angle = 51.6°) and offset so that one of the dimethylamino methyls sits over the fulvene π -system of a neighboring molecule.

E. Effect of Crystal Packing on Molecular Structure. In all cases, $\omega(\text{C}_6\text{C}_7)$ is smaller in the crystal than in the optimized structures, by 17–19° in **1**, **2**, and **3**(*Pca2₁*) and by 8–10° in **3**(*P2₁/c*) and **4**, a clear indication that the crystalline environment is more polarizing than the “gas phase”. The type-I alignment of aryl rings appears to be a more polarizing intermolecular interaction than the other types of packing arrangements encountered in **1–4**. The number of type-I interactions is also important. Thus, the four such interactions in

Table 11. Mulliken Charges for Monomer and Pentamer Structures of 2(*P2₁2₁2₁*) and 3(*Pca2₁*)^a

atom	$\rho(2(P2_12_12_1))$ monomer	$\rho(2(P2_12_12_1))$ pentamer ^b	$\Delta\rho(\text{pentamer}^b -$ monomer)	$\rho(3(Pca2_1))$ monomer	$\rho(3(Pca2_1))$ pentamer ^b	$\Delta\rho(\text{pentamer}^b -$ monomer)
N	-0.264	-0.264	-0.000	-0.263	-0.262	0.001
$\Sigma(C_1-C_5)$	-0.131	-0.145	-0.014	-0.119	-0.129	-0.010
C ₆	0.070	0.072	0.003	0.040	0.041	0.001
$\Sigma(C_1-C_6)$	-0.062	-0.073	-0.012	-0.079	-0.088	-0.009
$\Sigma(C_7-C_{12})$	0.061	0.057	-0.004	0.076	0.070	-0.006
C ₁₃	0.004	0.005	0.001			
$\Sigma(C_{13}-C_{18})$				0.015	0.015	-0.001
$\Sigma(NMe_2)$	-0.004	0.011	0.014	-0.013	0.004	0.016
$\Sigma(C_7-NMe_2)$	0.057	0.170	0.018	0.079	0.089	0.096
ρ_{tot}^c	-0.001	0.000	-0.001	-0.001	0.001	0.000

^a Charges include those of any attached hydrogen atoms. ^b These values are for the central molecule of the pentamer. ^c Total molecular charge.

3(*Pca2₁*) are more polarizing than the single interaction in **3**(*P2₁/c*), as evidenced by a smaller value of $\omega C_6 C_7$ in the former. Note that there are also four antiparallel intermolecular interactions in the X-ray structure of **2**.

To investigate whether type-A packing interactions between aryl rings do, in fact, shift electron density into the fulvene ring in **2** and **3**(*Pca2₁*), we calculated Mulliken charges at the HF/STO-3G level for both a single molecule and a pentamer consisting of a molecule surrounded by four neighbors arranged exactly as in the crystal lattice and with molecular geometries taken from the crystal structure. The Mulliken charges calculated for the monomer were then subtracted from the corresponding charges for the central molecule of the pentamer (Table 11). The total Mulliken electron density in the fulvene moiety (C₁-C₆) of the central molecule of the pentamer is increased by 0.0116 and 0.0093 electrons for **2** and **3**(*Pca2₁*), respectively, relative to the monomer. Thus, electron density is shifted from the (dimethylamino)-phenyl group into the fulvene ring of the central molecule of the pentamer with only a minimal basis set calculation and without any significant intermolecular charge transfer. Stabilization of the molecules in the pentamers of **2** and **3**(*Pca2₁*) of 0.63 and 0.89 kcal/mol, respectively, is found on comparing the total molecular energy of the monomers with the average total molecular energies for the corresponding pentamers.

It is of interest to consider the direction of polarization in the noncentrosymmetric crystals of **2** and **3**(*Pca2₁*). The fulvene rings of all of the molecules of **2** are tilted up along the *b* axis. In **3**(*Pca2₁*), the fulvene rings are tilted up along the *c* axis (Figures 3 and 5, respectively). We suggest that the polarization directions are along the *b* and *c* axes for **2** and **3**(*Pca2₁*), respectively, based solely on these structural observations.

NLO Properties. Compounds **1** and **5** have been shown to have exceptionally large molecular hyperpolarizability ($\mu\beta$) values.^{7a,d} Since a large molecular hyperpolarizability is a prerequisite for efficient second harmonic generation (SHG) in bulk materials, **1**-**5** represent an interesting series of compounds for solid-state studies.

Efficient SHG of bulk materials also depends on the orientation of the molecules in the crystal with respect to one another.¹⁴ If the molecules pack centrosymmetrically, as observed for **1**, **3**(*P2₁/c*), and **4**, the hyperpolarizabilities of the individual molecules cancel each other. However, if there is a unique axis resulting from noncentrosymmetric crystal packing, as in **2** and **3**(*Pca2₁*), then the hyperpolarizabilities of individual molecules may reinforce one another and lead to SHG. Noncen-

trosymmetric crystal packing does not guarantee SHG since molecular hyperpolarizabilities may accidentally cancel one another.²⁹

SHG was observed qualitatively in **2**, **3**(*Pca2₁*), and **5**. We made no attempt to quantify the NLO response in these materials, but it appears that the response in **5** is the largest and that in **3**(*Pca2₁*) is the smallest. The former result is in accord with previous measurements of $\mu\beta$.^{7a,d} Unfortunately, we were unable to grow crystals of **5** large enough to obtain a single crystal X-ray structure. It is likely that the fulvene and aryl rings are nearly coplanar based on comparison of the HF/6-31G-optimized steric environment at C₆ in **5** with that in **1**.

We also measured the UV-vis spectra of **3** and **5** as solutions in cyclohexane and as thin films cast from solution. For **3**, the long-wavelength absorption band (λ_{max}) appears at 393, 407, 404, 417-422, and 410-427 nm for a cyclohexane solution, benzene solution, methanol solution, and for multiple films cast from benzene and methanol, respectively.³⁰ (Recall that **3**(*P2₁/c*) and **3**(*Pca2₁*) were crystallized from benzene and methanol, respectively.) The shift to longer wavelength in the films relative to solution suggests less twist and an increase in π delocalization in the former. When contrasted with the greater value of λ_{max} for **3** in benzene relative to methanol, the small increase in λ_{max} for some films of **3** cast from methanol compared to benzene *might* reflect the observation that the fulvene and (dimethylamino)-phenyl rings of **3**(*Pca2₁*) are more nearly coplanar than those of **3**(*P2₁/c*). The later point is supported by ZINDO³¹ calculations using molecular geometries taken from the crystal structures of **3**(*P2₁/c*) and **3**(*Pca2₁*), where λ_{max} was calculated to be 338 and 342 nm, respectively. No SHG response was observed in any of the thin films.

Further, λ_{max} for **5** appears at 418, 415, 429 and 433 nm for solutions in cyclohexane, hexanes, benzene and a film cast from benzene, respectively.³⁰ (We were unable to cast a film of **5** from hexanes, the recrystallization solvent.) Because the absorbance of these films is small at 532 nm (the wavelength of the green light generated by doubling the frequency of the infrared laser output at 1064 nm), these compounds might be attractive candidates for NLO materials.

(29) Nicoud, J. F.; Twieg, R. J. *Nonlinear Optical Properties of Organic Molecules and Crystals*; Chemla, D. S., Zyss, J., Eds.; Academic Press: New York, 1987; Vol. 1, pp 246-7.

(30) The films cast for **3** and **5** were not characterized other than by UV-vis spectroscopy. The differences observed in λ_{max} may be due to differences in molecular order or to variations in film thickness.

(31) Zerner, M. C. *Rev. Comput. Chem.* **1991**, *2*, 313.

Summary

We have shown by comparison of geometry-optimized and X-ray structures that **1–4** are polarized on incorporation into the crystal lattice. Head-to-tail alignment of neighboring *p*-(dimethylamino)phenyl rings polarize π charge into the fulvene moiety to a greater extent than with other packing motifs. This effect is enhanced in the pentamer packing arrangement in **2** and **3**(*Pca2*₁) where a central *p*-(dimethylamino)phenyl ring is surrounded by four others aligned in the antiparallel direction. The increased polarization caused by pentamer-type packing is probably responsible for a decrease in ω (C₆C₇) in **3**(*Pca2*₁) relative to that in **3**(*P2*₁/*c*). Macroscopic nonlinear quadratic susceptibility (SHG) is reported for **2**, **3**(*Pca2*₁) and **5**, indicating the potential technological importance of this class of compounds.

Experimental Section

General Methods. IR spectra were recorded from KBr windows. UV-vis spectra were measured using spectrophotometric grade benzene and HPLC grade methanol and hexanes from Fischer Chemical Co. NMR spectra were recorded at 300 MHz for ¹H and 75 MHz for ¹³C. NMR solvents were used as received from Cambridge Isotope Laboratories. ¹H spectra were referenced to TMS, and ¹³C spectra were referenced to the solvent peak. Melting points are uncorrected. Elemental analyses were performed by Midwest Microlabs, Indianapolis, IN.

Synthesis. 6-(4-(Dimethylamino)phenyl)-6-methylfulvene (2) (mp 107–108 °C) was prepared by the method of Gugelchuk et al.^{6c}

6-(4-(Dimethylamino)phenyl)-6-phenylfulvene (3).³² Potassium hydroxide (1.883 g, 33.56 mmol) and 18-crown-6 (400 mg, 1.51 mmol) were dissolved in 50 mL of anhydrous THF and stirred in a foil-covered 250-mL round-bottomed flask under an argon atmosphere while 1.85 mL (1.5 g, 23 mmol) of freshly distilled cyclopentadiene was added dropwise. The reaction mixture was stirred for 30 min, and then 4.5 g (20 mmol) of 4-(dimethylamino)benzophenone in 15 mL of THF was added dropwise and the reaction mixture was stirred at room temperature for 22 h. The reaction mixture was then quenched with 75 mL of 3 M HCl and extracted with 3 × 50 mL of ethyl ether, and the combined organic layers were washed with 50 mL of brine and dried (Na₂SO₄). A solid black residue obtained on removal of the solvent was crushed and washed with ether. The crude product was then dissolved in methylene chloride and chromatographed on 80 g of silica gel with 5:1 pentane/methylene chloride. The product was crystallized from the eluant to afford 96 mg (5%) of **3** as orange crystals: mp 118–119.5 °C; ¹H NMR (CDCl₃) δ 7.3–7.5 (m, 5 H), 7.24 (m, 2 H), 6.69 (apparent d, 2 H, *J* = 9.0 Hz), 6.63–6.60 (m, 1 H), 6.57–6.54 (m, 1 H), 6.49–6.46 (m, 1 H), 6.22–6.17 (m, 1 H), 3.03 (s, 6 H); ¹³C NMR (CDCl₃) δ 153.4, 150.8, 141.9, 141.5, 134.2, 132.4, 130.9, 130.3, 128.8, 128.5, 127.4, 124.4, 124.1, 111.0, 40.2. IR (KBr) 2891, 1526, 1360 cm⁻¹; UV-vis (cyclohexane) λ_{\max} = 393 nm (ϵ = 9700), 298 (5600), 267 (7500). Anal. Calcd for C₂₀H₁₉N: C, 87.87; H, 7.01. Found: C, 87.72; H, 7.04.

(E)-6-(2-(4-(Dimethylamino)phenyl)ethenyl)fulvene (5).³³ A 500-mL three-necked round-bottomed flask fitted with a condenser and an addition funnel was charged with 3.0 mL (2.4 g, 36 mmol) of freshly distilled cyclopentadiene, 1.0 g (43 mmol) of Na, and 30 mL of MeOH under N₂. (*E*)-4-*N,N*-Dimethylaminocinnamaldehyde (2.055 g, 11.72 mmol) in 400 mL of MeOH was added dropwise, and the stirred solution turned orange. After 2 h, the reaction mixture was quenched with water, extracted with 3 × 100 mL of ether, dried (MgSO₄),

and concentrated to afford a red solid. The crude product was chromatographed on silica gel with 3:1 methylene chloride/hexanes to afford 150 mg (6%) of **5** as fine red needles, mp = 142–143 °C; TLC (3:1 methylene chloride/hexanes) *R*_f = 0.70; ¹H NMR (CDCl₃) δ 7.5–6.2 (m, 11 H), 3.02 (s, 6 H); ¹³C NMR (CDCl₃) δ 150.9, 143.4, 141.5, 139.4, 131.8, 130.1, 128.9, 125.0, 124.6, 121.6, 118.1, 112.0, 111.5, 108.3, 40.2; IR (KBr) 2856, 1581, 1364 cm⁻¹; UV-vis (cyclohexane) λ_{\max} = 418 nm (ϵ = 72 500). Anal. Calcd for C₁₆H₁₇N: C, 86.05; H, 7.67; N, 6.27. Found: C, 85.75; H, 7.65; N, 6.24.

Crystal Growth. Compound **2** was crystallized as dark orange square plates by slow evaporation of an isopropylamine solution. The crystal used for the X-ray structure determination of **3**(*P2*₁/*c*) was grown as orange blades by slow evaporation of a solution in acetone. Polymorph **3**(*P2*₁/*c*) was also crystallized from benzene and isopropylamine and found to have the same crystal habit and unit cell dimensions as the crystals grown from acetone. Polymorph **3**(*Pca2*₁) was grown by very slow evaporation of a methanol solution. A saturated solution of **3** in methanol was prepared and placed into a test tube that was then capped with a rubber septum and a syringe needle inserted. The test tube was left to stand for several months during which time very fine needles no thicker than 0.1 mm were formed.

Data Collection. Data for **2** and **3**(*P2*₁/*c*) were collected on a Siemens P3 diffractometer, in the ω scan mode with ω scan widths = 1°, variable ω scan speed 4–20 deg min⁻¹ and graphite-monochromated Mo-K α radiation (0.71073 Å). Data for **3**(*Pca2*₁) were collected on a Rigaku AFC5R diffractometer in the $\omega/2$ Å mode with ω scan widths = 1°, variable ω scan speed 4–20 deg min⁻¹ and nickel-filtered Cu-K α radiation (1.541 78 Å).

Structure Analysis and Refinement. All structures were solved by direct methods. Full-matrix least-squares refinements were carried out with all nonhydrogen atoms anisotropic and hydrogens in calculated positions. Structure solutions and refinements were performed on either a Silicon Graphics workstation or a Gateway PC computer using SHELXS³⁴ and SHELXL³⁵ in the Siemens crystal structure solution package. Atomic positions for **1**, **4**, and **9–12** were obtained from the CSD.¹⁵ The coordinate files were read into ORTEP-3.³⁶ Packing diagrams for **2**, **3**(*P2*₁/*c*), and **3**(*Pca2*₁) were generated using Ortep-3,³⁶ whereas those for **4** were generated using PLUTO.³⁷

Molecular Orbital Calculations. Ab initio molecular orbital geometry optimizations of **1–8** were performed at the Hartree-Fock level using the GAUSSIAN92¹⁰ and GAUSSIAN-94W¹¹ series of programs with the 6-31G¹² basis set. All geometry optimizations were checked by analytical frequency analysis in order to confirm that a true minimum had been found.

NLO Studies. Crystals of **2**, **3**(*Pca2*₁), or **5** were ground with an agate mortar and pestle and a sample was placed between two glass slides that were then held in a Nd:YAG laser beam. Thin films were prepared by placing a drop of a solution of **3** or **5** onto a quartz slide and allowing the solvent to evaporate.

Acknowledgment. We thank Dr. Steven Gieb for his assistance with data collection for the X-ray structures reported herein. This work was supported by the Petroleum Research Fund, administered by the American Chemical Society. Most of the calculations were performed on a computer donated to Carnegie Mellon University by the Intel Corp. We also express our thanks to Prof. Gary Patterson at Carnegie Mellon

(34) Sheldrick, G. M. *Acta Crystallogr.* **1990**, *A46*, 467.

(35) Sheldrick, G. M. SHELXL-93, A Program for Crystal Structure Refinement, University of Göttingen, 1993.

(36) ORTEP-3 for Windows: Farrugia, L. J. *J. Appl. Cryst.* **1997**, *30*, 565.

(37) PLUTO is part of the package of programs provided with the Cambridge Structural Database software.

(32) Nesmeyanov, A. N.; Sazonova, V. A.; Drozd, V. N.; Rodionova, N. A.; Zudkova, G. I. *Bull. Acad. Sci. USSR, Div. Chem. Sci. (Engl. Trans.)* **1965**, 2029.

(33) No synthetic details for **5** were reported by Kawabe et al. (ref 7a).

University and Prof. David Pratt at the University of Pittsburgh for assistance with the NLO experiments.

Supporting Information Available: Tables of atomic coordinates, bond lengths, and bond angles for the X-ray structures of **2**, **3**($P2_1/c$), and **3**($Pca2_1$). Atomic coordinates for

the calculated structures of **1-8**. π -Charges (HF/6-31G//HF/6-31G) for calculated structures of **1-8** and also for **2** (HF/6-31G//X-ray). This material is available free of charge via the Internet at <http://pubs.acs.org>.

JO990931X